Nonlocal Shear Stress for Homogeneous Fluids

B. D. Todd,[1,*] J. S. Hansen,[1] and Peter J. Daivis[2]

[1]*Centre for Molecular Simulation, Swinburne University of Technology, PO Box 218, Hawthorn, Victoria 3122, Australia*
[2]*Applied Physics, School of Applied Sciences, RMIT University, GPO Box 2476V, Melbourne, Victoria 3001, Australia*

(Received 8 November 2007; published 13 May 2008)

It has been suggested that for fluids in which the rate of strain varies appreciably over length scales of the order of the intermolecular interaction range, the viscosity must be treated as a nonlocal property of the fluid. The shear stress can then be postulated to be a convolution of this nonlocal viscosity kernel with the strain rate over all space. In this Letter, we confirm that this postulate is correct by a combination of analytical and numerical methods for an atomic fluid out of equilibrium. Furthermore, we show that a gradient expansion of the nonlocal constitutive equation gives a reasonable approximation to the shear stress in the small wave vector limit.

DOI: 10.1103/PhysRevLett.100.195901 PACS numbers: 66.20.−d, 02.70.Ns, 47.10.ab, 47.10.ad

It has been suggested that, in the linear regime, when the variation in the strain rate of a fluid is of the order of the range of intermolecular correlations, the local Newtonian law of viscosity relating the shear stress to the strain rate via a constant (local) viscosity will break down [1]. This has certainly been observed in systems of confined fluids where the strain rate can vary rapidly within several molecular diameters [2–6]. In the case of homogeneous unconfined fluids, it has also been suggested that the solution to this problem is to use a generalized form of the Navier-Stokes equations, in particular, one that invokes a nonlocal constitutive equation relating the shear stress to the strain rate [1]. In this formulation, one expresses the shear stress as a convolution of a nonlocal viscosity kernel with the strain rate. It was earlier pointed out by Alley and Alder [7] that such a kernel is just the Fourier transformed generalized transport coefficient in real space, and that such transport coefficients can be computed via generalized hydrodynamics [7–13]. While generalized hydrodynamics has been used to compute these kernels in reciprocal space, their applications have largely been limited to studying liquid structure and dynamics via neutron scattering or various autocorrelation functions [7,14]. Alley and Alder point out that generalized hydrodynamic models could be enormously useful and that once the generalized transport kernels are computed for a given fluid, they can be used in a variety of hydrodynamic applications at molecular length scales. Such problems could include studying the stress response of fluids experiencing shock waves [7,15–18], for example. In these cases, moment expansions commonly used in gas kinetic theory are usually applied [11,13]. Expansions of this type, including gradient expansions, have a limited range of applicability, as we will show later. It is therefore desirable to consider the entire nonlocal transport kernel, as we do in this Letter. A nonlocal constitutive equation, expressed as a gradient expansion, was used by Dhont [19] to explain shear-banding phenomena, and Masselon *et al.* [20] have very recently used the same type of constitutive equation to describe the effect of nonlocality on the velocity profile for Poiseuille flow of micellar solutions. A further potential application is in highly confined fluid flow. It is yet to be demonstrated whether such an approach can be successfully applied to fluids confined to molecular dimensions due to large density variations in the fluid [21,22], though we note that nonlocal constitutive equations have been used in the modelling of stress in Brownian suspensions of rigid fibers [23]. Similarly, it has recently been demonstrated that classical continuum elasticity models break down at small length scales where nonlocal behavior becomes important [24].

Despite the promise of using nonlocal hydrodynamic models at the molecular length scale, in particular, for the prediction of thermodynamic fluxes and their use in generalized Navier-Stokes or Fourier-like equations, we are unaware of any conclusive proof that such constitutive models will actually work, or any quantification of the range of their applicability. In this Letter, we address this shortfall by simulating a system of atoms interacting via a purely repulsive short ranged truncated and shifted Lennard-Jones (Weeks-Chandler-Andersen, WCA) potential [25] under the influence of a weak sinusoidal transverse force (STF) such that the fluid density remains constant in space and the fluid is thermostatted at constant temperature. Thus, as the fluid is strictly in the Newtonian regime where shear-thinning can be neglected, the only variations in the fluid viscosity are due to variations in the wavelength of the driving force and hence variations in the k-dependent viscosity (i.e., the nonlocal viscosity). By varying the wavelength of the spatially oscillatory field, while keeping all other parameters constant, we are able to test the validity of either the local or nonlocal constitutive models for the shear stress by deriving exact analytic expressions and comparing these predicted stresses with exact stresses computed directly from the simulation data.

In the case of a homogeneous fluid in a steady state in which variations in the strain rate are of the order of the width of the kernel $\eta(y)$ (i.e., the correlation length), the nonlocal linear constitutive expression for the shear stress

σ_{yx} is [1,7]

$$\sigma_{yx}(y) = \int_{-\infty}^{\infty} dy' \eta(y - y')\dot{\gamma}(y'). \quad (1)$$

In this expression, the flow geometry is such that the fluid flows in the x-direction with a velocity gradient in the y-direction. We note that for strong flows, nonlinear viscoelasticity becomes important, in which case this simple linear constitutive equation is invalid. We do not consider nonlinear constitutive equations in this Letter.

Consider a three-dimensional fluid flowing in the x-direction under the influence of a sinusoidally varying field $F_x(y) = F_0 \cos k_n y$ in the y-direction, as depicted in Fig. 1, where $k_n = 2\pi n/L_y$ and L_y is the length of the simulation box in the y-direction. If the force is sufficiently small such that the density ρ_0 of the fluid remains constant and the fluid is in the Newtonian regime (i.e., no shear-thinning occurs), then the shear stress can be computed exactly by integrating the governing momentum continuity equation, and can be readily shown to be [26,27]

$$\sigma_{yx}(y) = -\frac{F_0\rho_0}{k_n} \sin k_n y. \quad (2)$$

The streaming velocity is only excited to the first harmonic in the weak field limit and is given by

$$u_x(y) = \tilde{u}_x(k_n) \cos(k_n y) \quad (3)$$

where $\tilde{u}_x(k_n)$ is the first Fourier coefficient of the series. Differentiating with respect to y gives the strain rate as

$$\dot{\gamma}_x(y) = -k_n \tilde{u}_x(k_n) \sin(k_n y). \quad (4)$$

We have shown [26] that it is possible to compute the full inhomogeneous viscosity kernel from correlation functions of the transverse momentum current via equilibrium molecular dynamics simulations or directly from the STF method. Both methods lead to identical results. In that paper, we parameterized the kernel for the WCA fluid and found that a useful form could be given by the sum of two Gaussians, namely

$$\eta(y) = \frac{\eta_0}{2\sqrt{2\pi}}[\sigma_1 e^{-(\sigma_1 y)^2/2} + \sigma_2 e^{-(\sigma_2 y)^2/2}]. \quad (5)$$

η_0 is the effective viscosity of the liquid and is given by the integral of Eq. (5), and σ_1 and σ_2 are parameters that depend on density and temperature.

We can now analytically compute the predicted shear stress using both local and nonlocal linear constitutive models. In the former case, we use Newton's constitutive equation $\sigma^L_{yx}(y) = \eta_0 \dot{\gamma}(y)$ to give

$$\sigma^L_{yx}(y) = \eta_0 \tilde{\dot{\gamma}}_0 \sin k_n y \quad (6)$$

where $\tilde{\dot{\gamma}}_0 = -k_n \tilde{u}_x(k_n)$. Similarly, by substituting Eqs. (4) and (5) into Eq. (1), we find for the latter

$$\sigma^{\mathrm{NL}}_{yx}(y) = \frac{\eta_0 \tilde{\dot{\gamma}}_0}{2}[e^{-(k_n/\sqrt{2}\sigma_1)^2} + e^{-(k_n/\sqrt{2}\sigma_2)^2}] \sin k_n y. \quad (7)$$

These two predictive analytic expressions for the local and nonlocal shear stress can now be explicitly tested against precise numerical values for the shear stress computed from Eq. (2). Our expectation is that Eqs. (6) and (7) should give close to identical results when the spatial variation of $\dot{\gamma}(y)$ is negligible over the width of the kernel given by Eq. (5), and both these predictions should agree with the measured simulation stress computed via Eq. (2). However, when $\dot{\gamma}(y)$ varies appreciably over the length scale of the kernel, we expect Eq. (6) to break down, whereas Eq. (7) should predict the correct stress.

To test out these predictions, we performed nonequilibrium molecular dynamics (NEMD) simulations of the STF system depicted in Fig. 1, where we note that the system is infinitely periodic in all three dimensions. The simulations were performed on a fluid of 1700 atoms interacting via the WCA potential. The length of the simulation box in the y-direction was $L_y = 17.61$. Details of the simulations, including the equations of motion and thermostatting mechanism to constrain the temperature, are given in [26]. The parameters used in the simulations and calculations are all presented in Table I. We stress here that the kernel was computed by *independent* equilibrium MD simulations of the correlation function for the transverse momentum current, whereas the zero-wave-vector viscosity was computed by the standard Green-Kubo relation. The reader is referred to [26] for details of the kernel calculations.

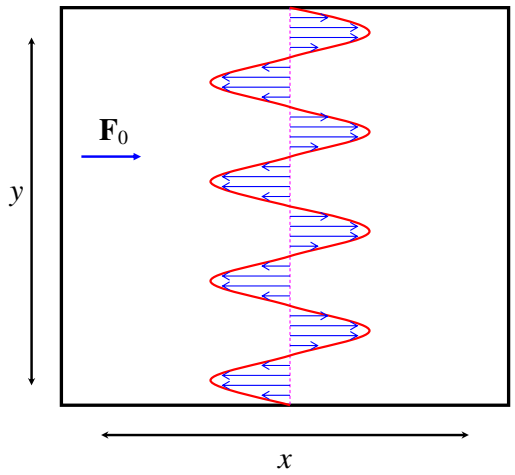

FIG. 1 (color online). Schematic representation of the STF simulation cell.

TABLE I. Parameters used in the computation of shear stress.

	T	ρ_0	F_0	η_0	σ_1	σ_2	k_n	$\tilde{u}_x(k_n)$
$n = 1$	0.765	0.685	0.15	0.929	1.929	4.497	0.357	0.886
$n = 10$	0.765	0.685	0.225	0.929	1.929	4.497	3.57	0.027

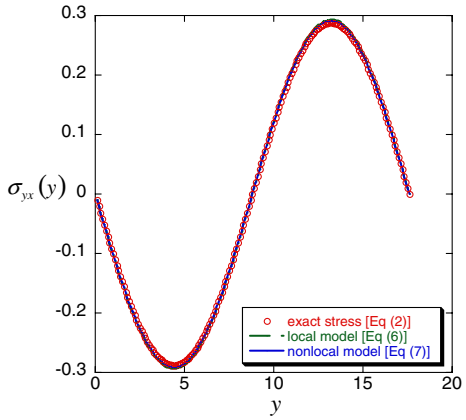

FIG. 2 (color online). Comparison of exact shear stress computed by Eq. (2) (circles), with the predictions obtained from the local constitutive model [dashed line, corresponding to Eq. (6)] and nonlocal model [full line, corresponding to Eq. (7)]. The excitation force has a long wavelength equal to the length of the simulation box in the y-direction and corresponds to a wave number $n = 1$.

In Fig. 2, we present the measured stress [Eq. (2)] with the local and nonlocal predictions given by Eqs. (6) and (7), respectively, for a system with the longest wavelength of the excitation force ($\lambda = L_y = 17.61$). The wave number n is 1, which gives $k_n = 0.357$. In this case, the variation of $\dot{\gamma}(y)$ over the range of the kernel (base width, $\zeta \sim 3$) is negligible ($\zeta/\lambda \sim 0.17$). As expected, we find that both the local and nonlocal predictions for the shear stress are identical and in excellent agreement with Eq. (2).

This result is now contrasted with the situation where $\dot{\gamma}(y)$ does vary appreciably over the kernel range (now $\zeta/\lambda \sim 1.7$). In this case, $n = 10$ and $\lambda = 1.76$ ($k_n = 3.57$). The predicted and measured stresses are displayed in Fig. 3. Clearly, we see that the local prediction fails badly, whereas the nonlocal prediction agrees perfectly with the measured stress. If we define the difference between the two predictive stresses as $\Delta\sigma_{yx}(y) \equiv \sigma^{L}_{yx}(y) - \sigma^{\mathrm{NL}}_{yx}(y)$, we have

$$\Delta\sigma_{yx}(y) = \sigma^{L}_{yx}(y)\left\{1 - \frac{1}{2}[e^{-(k_n/\sqrt{2}\sigma_1)^2} + e^{-(k_n/\sqrt{2}\sigma_2)^2}]\right\}. \tag{8}$$

This expression shows that, for a fixed point y in space, the error between the local and nonlocal predictive stresses increases rapidly with increasing k_n and then plateaus. We plot the term in curly brackets, which we call the error term, Δ, in Fig. 4. As an example, the error in the Newtonian (i.e., Navier-Stokes) approximation reaches 10% when the wavelength of the driving field decreases to approximately 2π in reduced units. In the limit as $k_n \to \infty$, the nonlocal stress tends to zero. This is also clearly seen by examining the exact expression for the measured

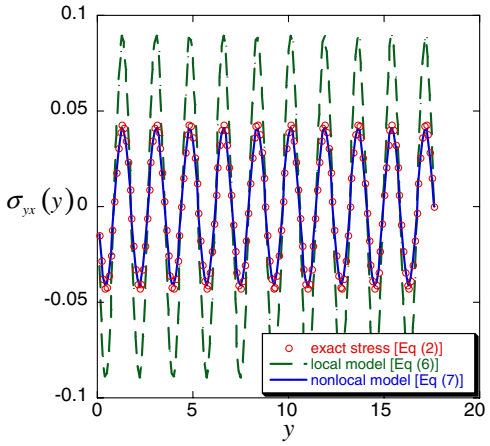

FIG. 3 (color online). As with Fig. 2, but now for a much shorter excitation wavelength corresponding to $n = 10$.

stress, given by Eq. (2), but cannot be predicted by the local Newtonian expression [Eq. (6)]. The amplitude of the shear stress decreases rapidly as a function of wave vector because at small wavelengths $\lambda \ll \zeta$, the variations in strain rate occur on length scales so much smaller than the width of the kernel that the kernel spans at least an entire wavelength of the strain rate. This in turn implies that the weighted contribution of the strain rate is zero. Because of space restrictions, we have only shown results for one state point at high fluid density; however, we have performed the same analysis at a number of fluid state points, and the results are all similarly convincing. We note that the problem could easily be inverted. By knowing what the exactly measured shear stress is [via Eq. (2)], we could predict the streaming velocity profile by substituting the Fourier transform of Eq. (1) into a generalized Navier-Stokes equation, finding the solution in k-space and inverse transforming the solution into real space.

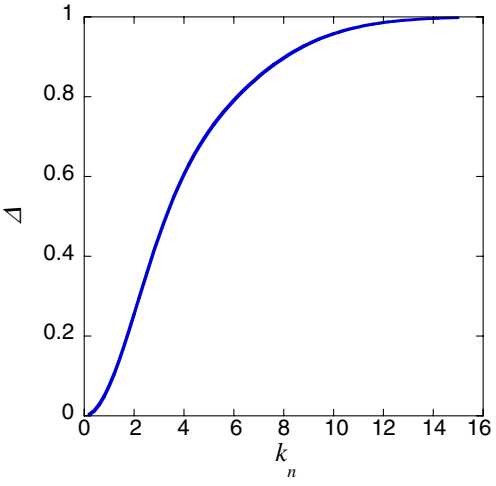

FIG. 4 (color online). Error term $\Delta = 1 - \frac{1}{2}[e^{-(k_n/\sqrt{2}\sigma_1)^2} + e^{-(k_n/\sqrt{2}\sigma_2)^2}]$ as a function of k_n for the system studied.

Finally, we note that Eq. (1) can be expanded about the strain rate at $y = y'$ in a Taylor series. Alternatively, one could take the Fourier transform of Eq. (1) and expand in k-space about $\tilde{\eta}(k)$, assuming that the kernel in reciprocal space is analytic about $k = 0$. Inverse transforming back into real space gives the expansion of the shear stress. Either method gives the same expression, which we present up to second order:

$$\sigma_{yx}(y) = \eta_0 \dot{\gamma}(y) + \eta_1 \frac{d\dot{\gamma}}{dy'}\bigg|_{y'=y} + \eta_2 \frac{d^2\dot{\gamma}}{dy'^2}\bigg|_{y'=y} + \cdots \tag{9}$$

where η_0 is as defined above, $\eta_1 = -\int_{-\infty}^{\infty} y\eta(y)dy = 0$ and $\eta_2 = \frac{1}{2}\int_{-\infty}^{\infty} y^2\eta(y)dy$. For our particular system (Fig. 1), Eq. (9) leads to

$$\sigma_{yx}(y) \approx \eta_0 \tilde{\dot{\gamma}}_0 \left[1 + \frac{1}{4}\left(\frac{1}{\sigma_1^2} + \frac{1}{\sigma_2^2}\right)k_n^2\right] \sin k_n y. \tag{10}$$

In the case of the lowest wave vectors $n = (1, 2)$ and a force of $F_0 = (0.15, 0.225)$, with values of $k_n = (0.357, 0.714)$, the coefficient of the stress given by Eq. (10) is $(-0.296, -0.236)$. This compares well with the exact values of -0.288 and -0.216 computed via Eq. (2) and confirms that the gradient expansion can be a useful approximation to the stress for small wave vectors. For example, a 10% deviation in stress computed from the gradient expansion and the exact nonlocal kernel is found when the wavelength of the driving field is approximately 8 in reduced units (cf. the value of 2π where the Navier-Stokes approximation gives the same deviation as shown above).

We gratefully acknowledge the Australian Research Council for Discovery Grant No. DP0663759 to support this project.

*Corresponding author: btodd@swin.edu.au

[1] D. J. Evans and G. P. Morriss, *Statistical Mechanics of Nonequilibrium Liquids* (Academic Press, London, 1990).
[2] E. Akhmatskaya *et al.*, J. Chem. Phys. **106**, 4684 (1997).
[3] I. Bitsanis, J. Chem. Phys. **93**, 3427 (1990).
[4] E. Manias, G. Hadziioannou, and G. ten Brinke, Langmuir **12**, 4587 (1996).
[5] K. P. Travis and K. E. Gubbins, J. Chem. Phys. **112**, 1984 (2000).
[6] K. P. Travis, B. D. Todd, and D. J. Evans, Phys. Rev. E **55**, 4288 (1997).
[7] W. E. Alley and B. J. Alder, Phys. Rev. A **27**, 3158 (1983).
[8] N. K. Ailawadi, A. Rahman, and R. Zwanzig, Phys. Rev. A **4**, 1616 (1971).
[9] A. Z. Akcasu and E. Daniels, Phys. Rev. A **2**, 962 (1970).
[10] J. P. Boon and S. Yip, *Molecular Hydrodynamics* (McGraw-Hill, New York, 1980).
[11] B. C. Eu, *Generalised Thermodynamics: The Thermodynamics of Irreversible Processes and Generalized Hydrodynamics* (Kluwer, Dordrecht, 2002).
[12] D. Jou, J. Casas-Vazquez, and G. Lebon, *Extended Irreversible Thermodynamics* (Springer, Heidelberg, 2001).
[13] I. Muller and T. Ruggeri, *Rational Extended Thermodynamics* (Springer-Verlag, New York, 1998).
[14] W. E. Alley, B. J. Alder, and S. Yip, Phys. Rev. A **27**, 3174 (1983).
[15] B. L. Holian *et al.*, Phys. Rev. A **22**, 2798 (1980).
[16] B. L. Holian and P. S. Lomdahl, Science **280**, 2085 (1998).
[17] E. J. Reed *et al.*, Phys. Rev. E **74**, 056706 (2006).
[18] E. J. Reed, L. E. Fried, and J. D. Joannopoulos, Phys. Rev. Lett. **90**, 235503 (2003).
[19] J. K. G. Dhont, Phys. Rev. E **60**, 4534 (1999).
[20] C. Masselon, J.-B. Salmon, and A. Colin, Phys. Rev. Lett. **100**, 038301 (2008).
[21] P. J. Cadusch *et al.*, J. Phys. A **41**, 035501 (2008).
[22] B. D. Todd, Mol. Simul. **31**, 411 (2005).
[23] R. L. Schiek and E. S. G. Shaqfeh, J. Fluid Mech. **296**, 271 (1995).
[24] R. Maranganti and P. Sharma, Phys. Rev. Lett. **98**, 195504 (2007).
[25] J. D. Weeks, D. Chandler, and H. C. Andersen, J. Chem. Phys. **54**, 5237 (1971).
[26] J. S. Hansen *et al.*, Phys. Rev. E **76**, 041121 (2007).
[27] B. D. Todd, D. J. Evans, and P. J. Daivis, Phys. Rev. E **52**, 1627 (1995).